Upon integration equation (38) takes the form

$$u = Y - (N^{\circ}_{H_2O}/N_C)\left\{Y - \frac{2K^2}{2K-1} \ln \frac{2K+Y}{2K} - \frac{K-1}{2K-1} \ln (1+Y)\right\}. \quad (39)$$

When expressed in terms of fraction of steam decomposed, f, equation (39) becomes

$$u = \frac{f}{1-f} - (N^{\circ}_{H_2O}/N_C)\left\{\frac{f}{1-f} + \frac{2K^2}{2K-1} \ln \frac{2K}{2K-(2K-1)f} - (K+1) \ln \frac{1}{1-f}\right\}. \quad (40)$$

For complete mixing, integration of equation (36) leads to

$$Y = -K_2 - K_2k_3(C_t)\,W/N_C. \quad (41)$$

Application of Theory and Discussion of Results

DETERMINATION OF THE OXYGEN EQUILIBRIUM AND THE RATE CONSTANTS

Fraction of steam reacted is represented in figure 9 as a function of the ratio of the amount of coke sample to the inlet steam flow rate. For steam-coke reactions back mixing appeared to be less pronounced than in the case of carbon dioxide-carbon reactions. Lessening of the back mixing was further enhanced by the use of higher flow rates. The values of K_2 and $k_3(C_t)$ were determined by evaluating the function u using equation (40) and by graphical integration. At moderate conversions, u has been found to be insensitive to the values of water-gas shift equilibrium K between 0.4 and 0.8 which cover a temperature range of 900° to 1,200° C. When a value of 0.5 is used for K, equation (40) takes the simplified form

$$u = \frac{3(1+Y)^2}{Y(1+2Y)} \ln (1+Y) - \frac{3+4Y}{1+2Y}. \quad (42)$$

It thus became possible to construct a plot of u as a function of Y or fraction of steam reacted $f = Y/(1+Y)$, valid at temperatures between 900° and 1,200° C. The plot is shown in figure 10.

Graphical representation of u as a function of W/N_C leads to the values of K_2 and $k_3(C_t)$ as seen in figure 11 (see equation (36)). The circles shown in figure 11 are determined by this procedure. As will be shown, water-gas shift equilibrium was not attained under all conditions. It seemed, therefore, desirable to determine the values of the function u without recourse to an assumption of water-gas shift equilibrium, as is necessary for an analytical solution of equation (36). The values of u can be obtained graphically from a plot of Y against N_C if experiments are conducted at constant inlet steam flow rates with successively increasing amounts of coke. Otherwise, it becomes necessary to plot Y against $N_C/N^{\circ}_{H_2O}$ as shown in figure 12 for experiments conducted at 1,100° C. The areas under the curve between N_C or $N_C/N^{\circ}_{H_2O}=0$, and the value chosen on the abscissa yield the integral of YdN_C or $Yd(N_C/N^{\circ}_{H_2O})$ from which one calculates u directly. From a separate plot of W/N_C against N_C or $N_C/N^{\circ}_{H_2O}$, one can obtain the values of W/N_C corresponding to the values of abscissa chosen in graphical integration. Such a plot is shown in figure 13. The final plot involves the graphical representation of u against W/N_C as shown in figure 11. Graphical integration requires the drawing of arbitrary lines through the experimental points. Once the values of K_2 and k_3 (C_t) are determined, the lines drawn can be compared with those calculated using equations (42) and (36). In figure 12, the line drawn arbitrarily agreed well with that calculated. For the plot of figure 13, however, the line drawn arbitrarily could not be well reproduced by calculation. This was expected because the calculated curves in particular are dependent upon the value of the water-gas shift equilibrium used, as shown at the bottom of figure 13. The curve drawn for K=0 corresponds to the case when gasification products are CO and H_2, that for $K=\infty$ when products are CO_2 and H_2, and that for K=0.465 when water-gas shift equilibrium prevails. Comparison of these curves gives an idea about the effect of water-gas shift reaction upon the gasification rate of coke.

Graphically determined values of function of u are also included in figure 11 as crosses. It is seen that the analytical expressions yield reasonable values *despite* failure to attain water-gas shift equilibrium.

INFLUENCE OF PARTICLE SIZE

In experiments conducted at 1,000°, 1,100° and 1,200° C. several particle sizes were employed. As seen in figure 9, no trend in reaction rate was detectable with change in particle size, which ranged from 16–20 to 100–140 mesh. This fact suggests that film-boundary diffusion was not very important under the experimental conditions employed.

INFLUENCE OF INERT GAS

As in the case of carbon dioxide reaction, helium was introduced at successively increased

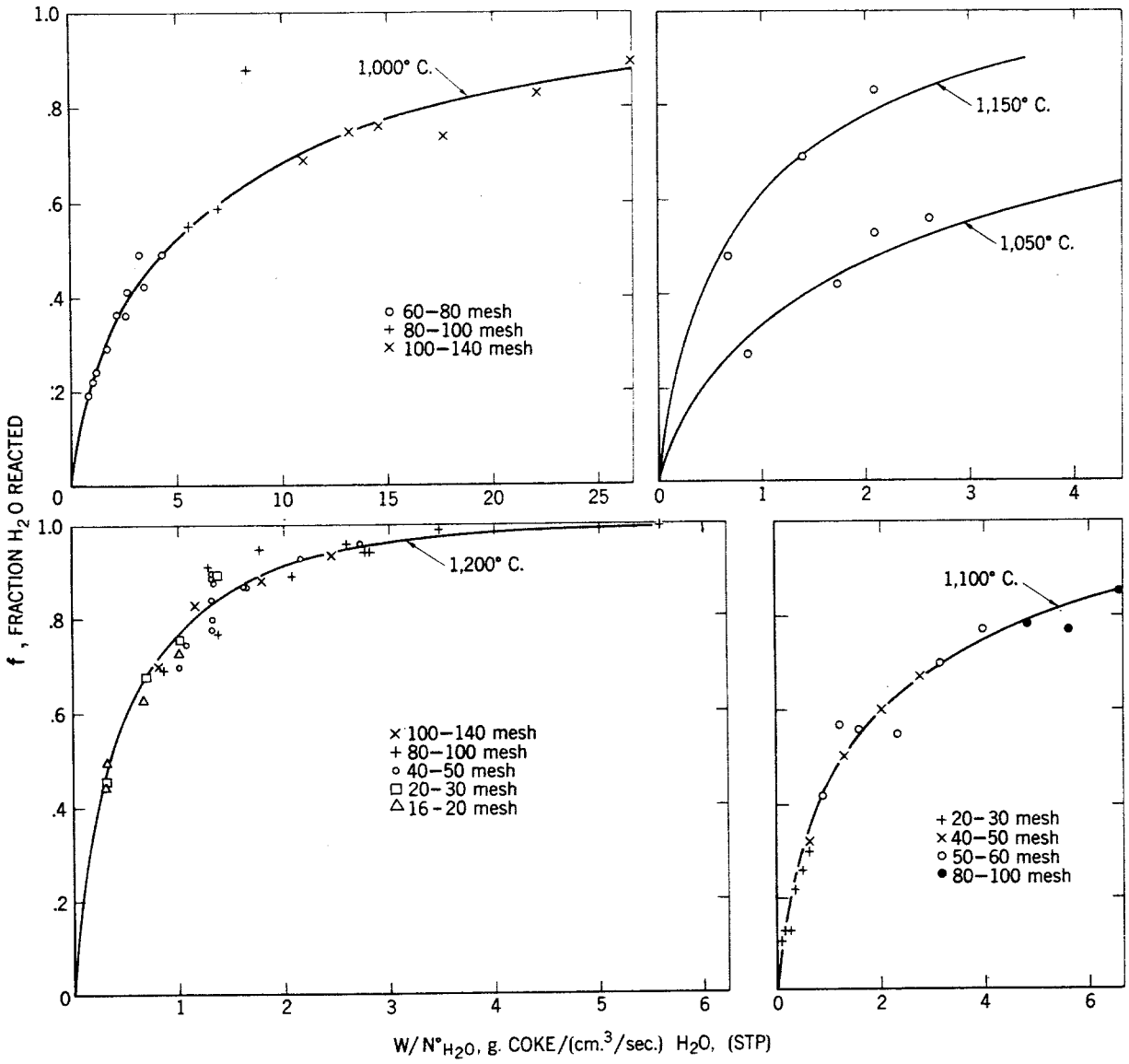

FIGURE 9.—Reaction of Steam With a Metallurgical Coke.

rates while keeping flow rate of reactant gas, that is steam, and the amount of coke constant. The results are tabulated in table 4 and represented graphically in figure 14. As seen from the figure, dilution of the gas phase, hence increase in space velocity, had no marked influence upon the reaction rate. This fact, coupled with the lack of dependence of reaction rate upon particle size, clearly demonstrates that the film boundary diffusion is extremely fast compared to the gasification rate. Figure 14 indicates a zero-order reaction with respect to partial pressure of steam; however, this is not the case as seen from the differential equation (equation (29)). As was the case in carbon dioxide-carbon reaction, partial pressure of steam and space velocity cannot be used indiscriminantly in formulating the heterogeneous reactions of steam with carbon because neither is an independent variable.

INFLUENCE OF SPACE VELOCITY

Influence of space velocity on the reaction of coke with steam was similar to that on the reaction of coke with carbon dioxide. Change of space velocity had no influence on the fraction of H_2O reacted if the change was effected by in-

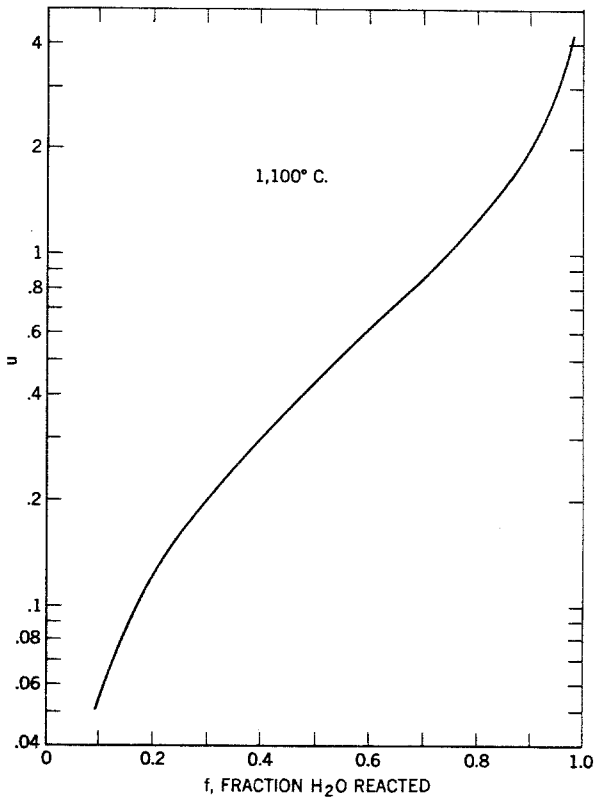

FIGURE 10.—Graphical Representation of Equation (40).

creasing flow rate of inert gas or if the ratio of the weight of coke to the inlet flow rate of steam was kept constant.

As in CO_2-coke reactions, a single curve can be constructed expressing the fraction of H_2O reacted as a function of $W/N^\circ_{H_2O}$ at any temperature. This is illustrated in figure 9. However, it is not possible to construct a single curve for the gasification rate N_C. The experiment conducted for investigating the role of partial pressure and space velocity clearly showed that gas-phase (film-boundary) diffusion had no influence on the reaction rate.

WATER-GAS SHIFT EQUILIBRIUM

The values of $(H_2)(CO_2)/(H_2O)(CO)$ are plotted in figure 15 against the fraction of water reacted. Solid lines drawn represent the equilibrum constant of the water-gas shift reaction. It is seen that the equilibrium is not attained at the lower temperatures when conversion of steam is low. The values plotted show considerable scatter, partly owing to somewhat poor reproducibility of data (figs. 9 and 13) and partly owing to errors in gas analysis as manifested in material balances at high steam conversion. As the concentration of steam diminishes, carbon dioxide concentration also diminishes, and slight errors in determining either or both lead to wide fluctuations in the values of $(H_2)(CO_2)/(H_2O)(CO)$. From figure 15, it may seem that an overshift in the reaction may also occur. Under the experimental conditions adopted in these studies an overshift could very well be caused by slight longitudinal mixing of gases, high escape velocity of hydrogen probably being the major cause.

The lack of attainment of water-gas shift reaction suggests that oxygen exchange reactions are not extremely fast at least not all of

TABLE 4.—*Influence of nitrogen on the reaction of steam with a high-temperature metallurgical coke* [1]

Run No.	N_2 rate [2]	Outlet gas composition, water-free basis, percent				f [3]	$N_C/N^\circ_{H_2O}$ [4]	$\frac{(H_2)(CO_2)}{(H_2O)(CO)}$
		CO_2	CO	H_2	N_2			
188	0. 269	10. 3	30. 6	49. 0	10. 1	0. 58	0. 486	0. 46
189	. 535	8. 4	28. 5	45. 5	17. 6	. 62	. 501	. 48
190	. 786	8. 2	26. 1	41. 7	24. 0	. 61	. 502	. 49
191	1. 06	7. 4	24. 2	38. 8	29. 6	. 62	. 504	. 50
192	1. 25	6. 9	22. 9	36. 3	33. 9	. 60	. 490	. 45
193	1. 49	6. 5	21. 7	34. 1	37. 6	. 60	. 498	. 45
194	1. 67	6. 0	21. 3	32. 9	39. 8	. 62	. 512	. 46
195	2. 12	6. 2	18. 2	29. 6	46. 0	. 60	. 502	. 51
196	2. 41	5. 5	17. 6	27. 4	49. 5	. 60	. 501	. 47
197	3. 11	5. 1	14. 7	23. 6	56. 6	. 58	. 486	. 48
198	3. 71	4. 6	12. 8	20. 7	61. 9	. 55	. 465	. 44
199	4. 35	4. 2	11. 9	19. 6	64. 3	. 59	. 486	. 51

[1] Temperature 1,100° C., particle size 40–50 mesh (U.S. standard), sample weight 5 g., H_2O rate 2.24 cm.³/sec.
[2] cm.³/sec. (STP).
[3] Fraction H_2O reacted (by hydrogen balance).
[4] g. atom C/g. mole H_2O.

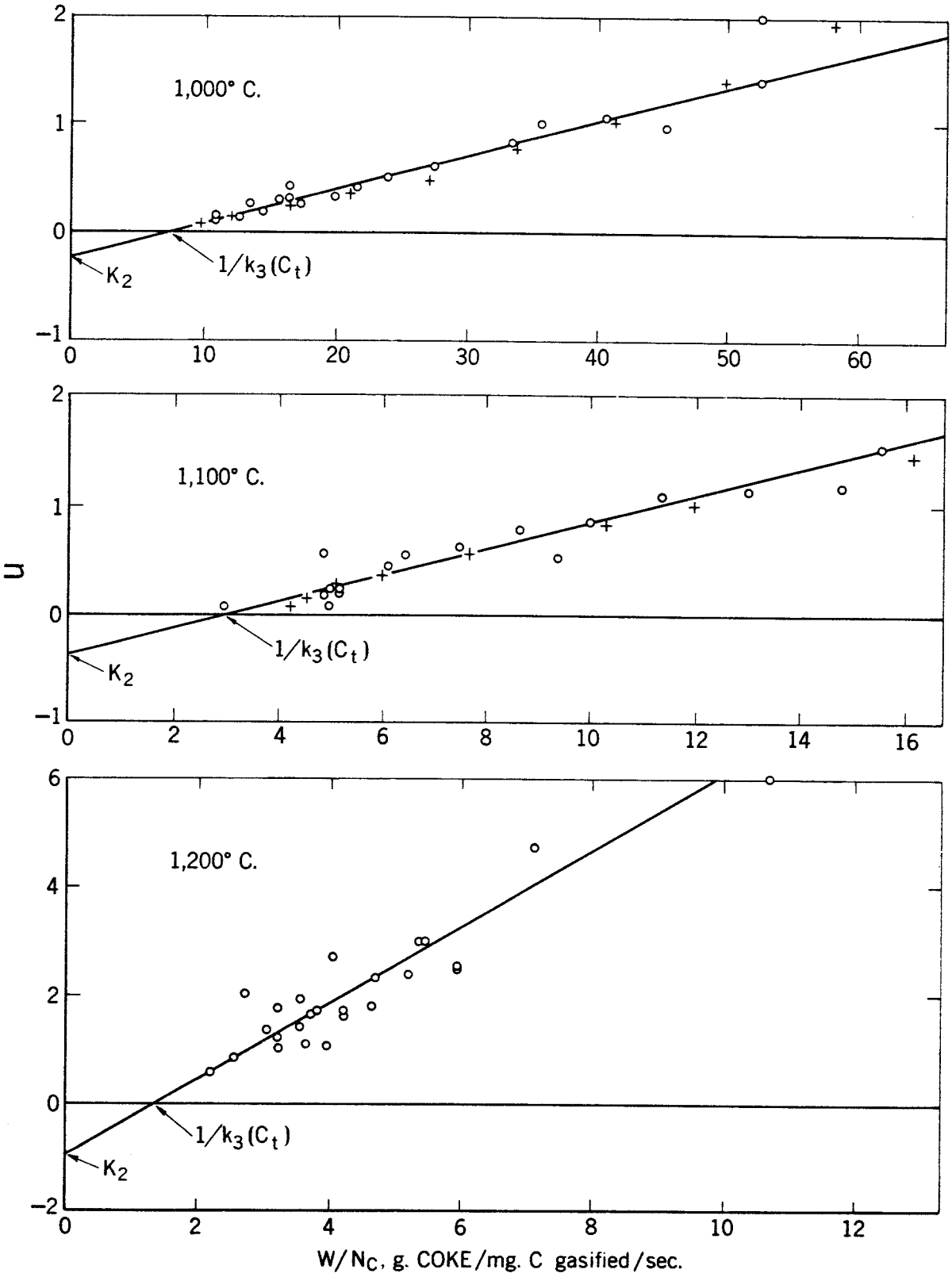

FIGURE 11.—Determination of the Parameters of the Reaction of Steam With a Metallurgical Coke.

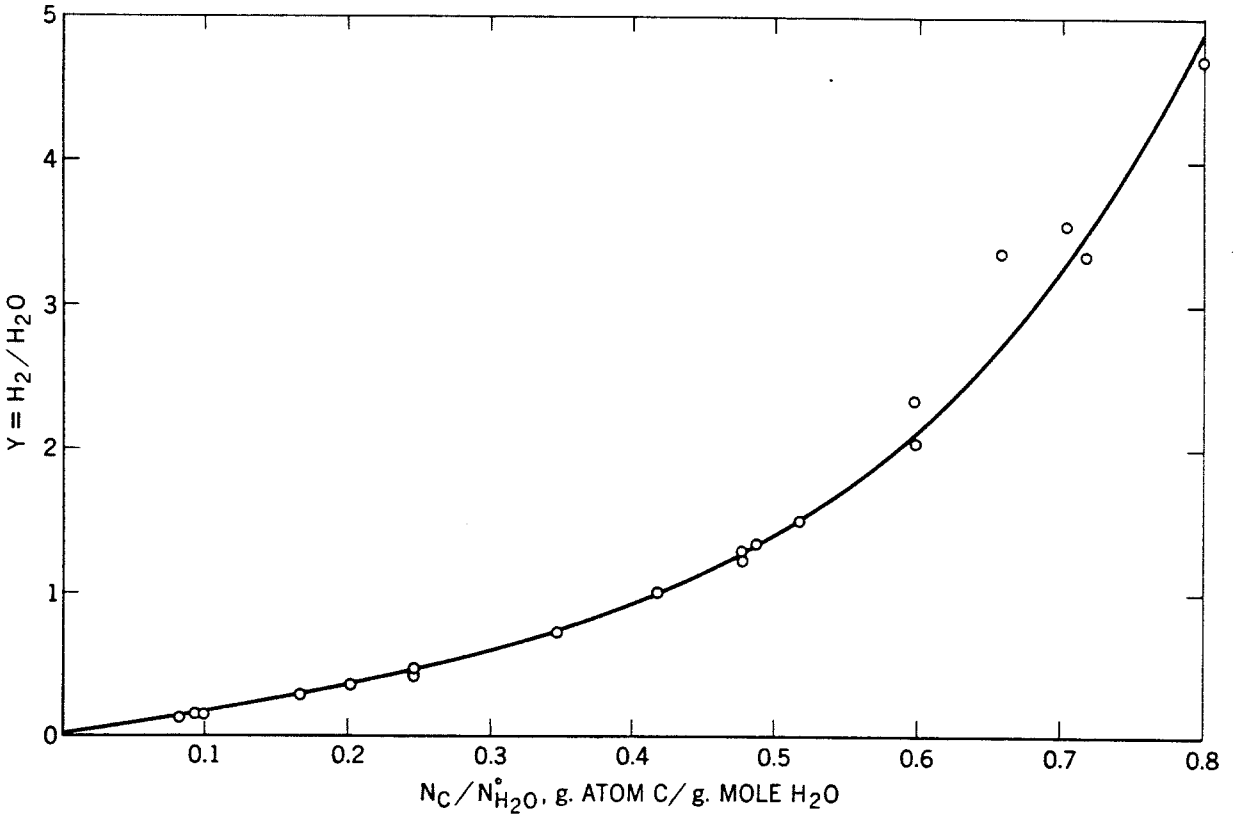

FIGURE 12.—Variation of Hydrogen-to-Steam Ratio With Total Carbon Gasified.

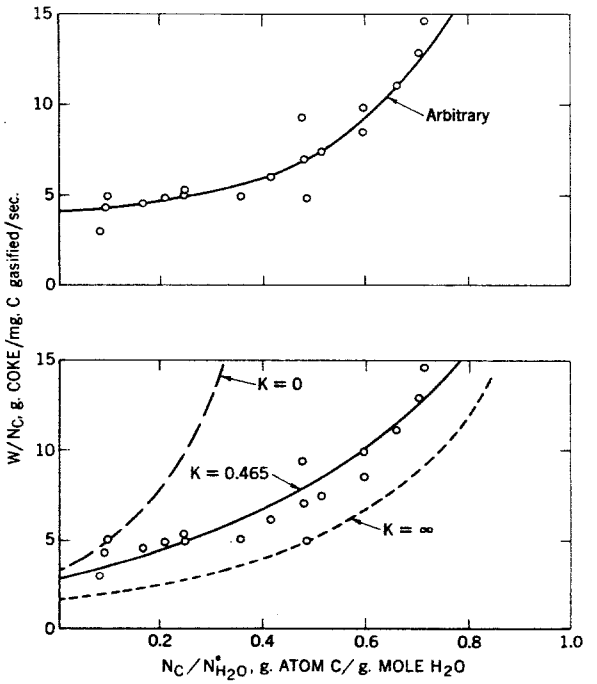

FIGURE 13.—Relation of Rate of Gasification to Weight of Carbon and Steam Flow Rate.

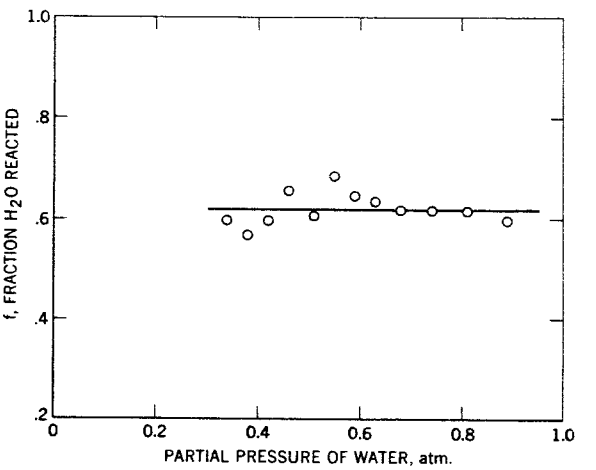

FIGURE 14.—Effect of Partial Pressure of Steam on Fraction of Steam Decomposed at Constant Flow Rate Steam. Partial pressure of steam was reduced by introduction of helium.

the four reactions involved. The equilibrium constants obtained would correspond to quasi-equilibria often obtained in kinetic analysis of consecutive reactions. Another explanation, not obvious from the analysis made thus far,

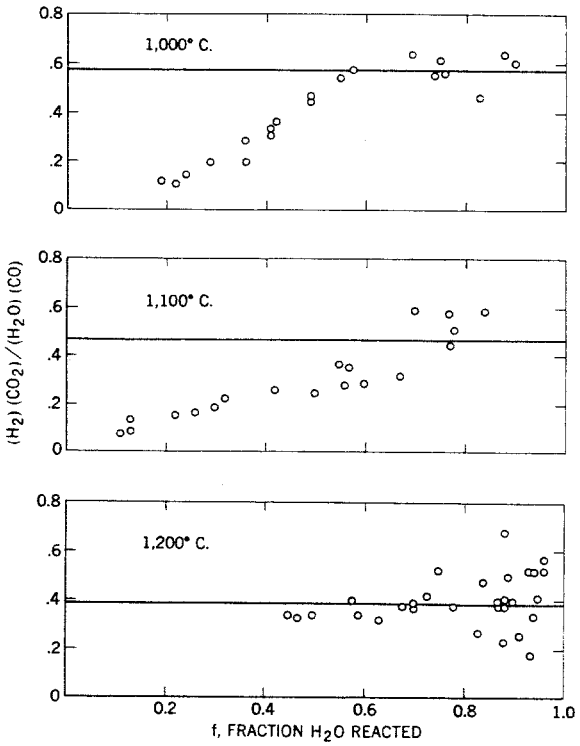

FIGURE 15.—Attainment of Water-Gas Shift Equilibrium as a Function of the Fraction of Steam Reacted.

is that some sort of hindering due to pore diffusion is present but is not manifested by dependence upon particle size nor upon inert gas concentration.

COMPARISON OF STEAM-COKE AND CARBON DIOXIDE-COKE DATA

The values of K_2 obtained from plots in figure 11 are shown in figure 16 against the reciprocal of the absolute temperature of reaction. As seen from equation (27), values of K_2 can be predicted from the values of K_1 obtained from carbon dioxide reactions, that is, $K_2=K_1K$. Values of K_2 obtained from carbon dioxide data (fig. 6) by the above relationship are also shown in figure 11 as a dotted line. The agreement seen in the figure is surprisingly good; it suggests that the quasi-equilibrium values may not be unreasonably different from true equilibrium values.

The values of $k_3(C_t)$, also obtained from plots shown in figure 11, are shown in figure 17 with those obtained from carbon dioxide reactions. It is seen that the slopes of the two lines are more or less parallel. Steam data are about 60 pct. higher than carbon dioxide data, indicating that the number of reaction sites is higher when steam is present in the gas phase. The absence

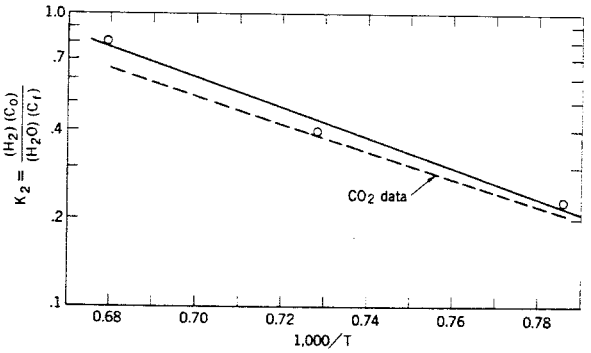

FIGURE 16.—Equilibrium Constant of the Oxygen Exchange Reaction Over Coke Between Steam and Hydrogen as a Function of Temperature.

of dependence of reaction rate upon particle size and upon inert gas concentration suggests that this increased number is probably the result of reaction sites being of more than one type; that is, terminal carbon atoms can be in different bonding and electronic states, and steam is capable of reacting with more types than carbon dioxide. However, if this explanation is valid, it would seem that the slopes of the $k_3(C_t)$ plots obtained from CO_2-coke and H_2O-coke reactions should not necessarily be the same. An alternate explanation, consistent with the lack of attainment of water-gas shift

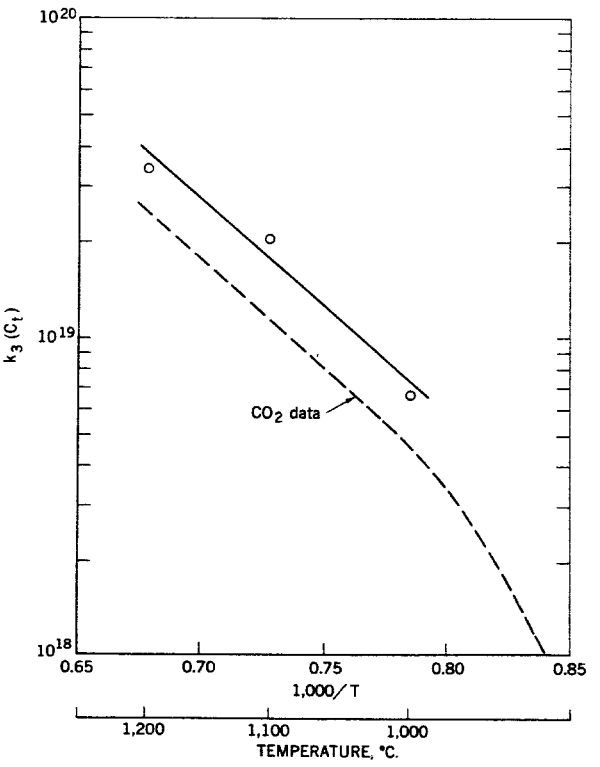

FIGURE 17.—Constants of the Gasification Step as a Function of Temperature.